LABORATORI NAZIONALI DI FRASCATI
SIS-Pubblicazioni

LNF-02/003(P)
10 APrile 2002
hep-ex/0204013

Study of the Decay $\phi \to \pi^0\pi^0\gamma$ with the KLOE Detector

The KLOE Collaboration*

Abstract

We have measured the branching ratio BR($\phi \to \pi^0\pi^0\gamma$) with the KLOE detector using a sample of $\sim 5 \times 10^7$ ϕ decays. ϕ mesons are produced at DAΦNE, the Frascati ϕ-factory. We find BR($\phi \to \pi^0\pi^0\gamma$)= $(1.09 \pm 0.03_{\rm stat} \pm 0.05_{\rm syst}) \times 10^{-4}$. We fit the two–pion mass spectrum to models to disentangle contributions from various sources.

PACS:13.65.+i;14.40.-n

Submitted to Elsevier Science for publication on Phys. Lett. B.

* The KLOE Collaboration

A. Aloisio[e], F. Ambrosino[e], A. Antonelli[b], M. Antonelli[b], C. Bacci[j], G. Bencivenni[b], S. Bertolucci[b], C. Bini[h], C. Bloise[b], V. Bocci[h], F. Bossi[b], P. Branchini[j], S. A. Bulychjov[o], G. Cabibbo[h], R. Caloi[h], P. Campana[b], G. Capon[b], G. Carboni[i], M. Casarsa[l], V. Casavola[d], G. Cataldi[d], F. Ceradini[j], F. Cervelli[f], F. Cevenini[e], G. Chiefari[e], P. Ciambrone[b], S. Conetti[m], E. De Lucia[h], G. De Robertis[a], P. De Simone[b], G. De Zorzi[h], S. Dell'Agnello[b], A. Denig[b], A. Di Domenico[h], C. Di Donato[e], S. Di Falco[f], A. Doria[e], M. Dreucci[b], O. Erriquez[a], A. Farilla[j], G. Felici[b], A. Ferrari[j], M. L. Ferrer[b], G. Finocchiaro[b], C. Forti[d], A. Franceschi[b], P. Franzini[h], C. Gatti[f], P. Gauzzi[h], S. Giovannella[b], E. Gorini[d], F. Grancagnolo[d], E. Graziani[j], S. W. Han[b,n], M. Incagli[f], L. Ingrosso[b], W. Kim[k], W. Kluge[c]C. Kuo[c], V. Kulikov[o], F. Lacava[h], G. Lanfranchi[b], J. Lee-Franzini[b,k], D. Leone[h], F. Lu[b,n], M. Martemianov[c], M. Matsyuk[b,o], W. Mei[b], L. Merola[e], R. Messi[i], S. Miscetti[b], M. Moulson[b], S. Müller[c], F. Murtas[b], M. Napolitano[e], A. Nedosekin[b,o], F. Nguyen[j], M. Palutan[j], L. Paoluzi[i], E. Pasqualucci[h], L. Passalacqua[b], A. Passeri[j], V. Patera[b,g], E. Petrolo[h], G. Pirozzi[e], L. Pontecorvo[h], M. Primavera[d], F. Ruggieri[a], P. Santangelo[b], E. Santovetti[i], G. Saracino[e], R. D. Schamberger[k], B. Sciascia[h], A. Sciubba[b,g], F. Scuri[l], I. Sfiligoi[b], T. Spadaro[h], E. Spiriti[j], G. L. Tong[b,n], L. Tortora[j], E. Valente[h], P. Valente[b], B. Valeriani[c], G. Venanzoni[f], S. Veneziano[h], A. Ventura[d], Y. Xu[b,n], Y. Yu[b,n], Y. Wu[b,n]

[a] *Dipartimento di Fisica dell'Università e Sezione INFN, Bari, Italy*
[b] *Laboratori Nazionali di Frascati dell'INFN, Frascati, Italy*
[c] *Institut für Experimentelle Kernphysik, Universität Karlsruhe, Germany*
[d] *Dipartimento di Fisica dell'Università e Sezione INFN, Lecce, Italy*
[e] *Dipartimento di Scienze Fisiche dell'Università "Federico Secondo" e Sezione INFN, Napoli, Italy*
[f] *Dipartimento di Fisica dell'Università e Sezione INFN, Pisa, Italy*
[g] *Dipartimento di Energetica dell'Università "La Sapienza", Roma, Italy*
[h] *Dipartimento di Fisica dell'Università "La Sapienza" e Sezione INFN, Roma, Italy*
[i] *Dipartimento di Fisica dell'Università "Tor Vergata" e Sezione INFN, Roma, Italy*
[j] *Dipartimento di Fisica dell'Università "Roma Tre" e Sezione INFN, Roma, Italy*
[k] *Physics Department, State University of New York at Stony Brook, USA*
[l] *Dipartimento di Fisica dell'Università e Sezione INFN, Trieste, Italy*
[m] *Physics Department, University of Virginia, USA*
[n] *Permanent address: Institute for High Energy Physics, CAS, Beijing, China*
[o] *Permanent address: Institute for Theoretical and Experimental Physics, Moscow, Russia*

The decay $\phi \to \pi^0\pi^0\gamma$ was first observed in 1998 [1]. Only two experiments have measured its rate [2,3]. The measured rate is too large if $\phi \to f_0(980)\gamma$, with $f_0 \to \pi^0\pi^0$, were the dominating contribution and f_0(980) is interpreted as a $q\overline{q}$ scalar state [4]. Possible explanations for the f_0 are: ordinary $q\overline{q}$ meson, $q\overline{q}q\overline{q}$ state, $K\overline{K}$ molecule [5–7]. Similar considerations apply also to the a_0(980) meson. The decay $\phi \to \pi^0\pi^0\gamma$ can clarify this situation since both the branching ratio and the line shape depend on the structure of the f_0. We present in the following a study of the decay $\phi \to \pi^0\pi^0\gamma$ performed with the KLOE detector [8] at DAΦNE [9], an e^+e^- collider which operates at a center of mass energy $W{=}M_\phi \sim 1020$ MeV. Data were collected in the year 2000 for an integrated luminosity $L_{\rm int} \sim 16$ pb^{-1}, corresponding to around 5×10^7 ϕ-meson decays.

The KLOE detector consists of a large cylindrical drift chamber, DC, surrounded by a lead-scintillating fiber electromagnetic calorimeter, EMC. A superconducting coil around the EMC provides a 0.52 T field. The drift chamber [10], 4 m in diameter and 3.3 m long, has 12,582 all-stereo tungsten sense wires and 37,746 aluminum field wires. The chamber shell is made of carbon fiber-epoxy composite and the gas used is a 90% helium, 10% isobutane mixture. These features maximize transparency to photons and reduce $K_L \to K_S$ regeneration and multiple scattering. The position resolutions are σ_{xy}~150 μm and σ_z~ 2 mm. The momentum resolution is $\sigma(p_\perp)/p_\perp \approx 0.4\%$. Vertices are reconstructed with a spatial resolution of ~3 mm. The calorimeter [11] is divided into a barrel and two endcaps, for a total of 88 modules, and covers 98% of the solid angle. The modules are read out at both ends by photomultipliers; the readout granularity is ~4.4×4.4 cm^2, for a total of 2440 cells. The arrival times of particles and the positions in three dimensions of the energy deposits are obtained from the signals collected at the two ends. Cells close in time and space are grouped into a calorimeter cluster. The cluster energy E is the sum of the cell energies. The cluster time T and position $\vec{R}$ are energy weighted averages. Energy and time resolutions are $\sigma_E/E = 5.7\%/\sqrt{E\ (\rm GeV)}$ and $\sigma_t = 57\ {\rm ps}/\sqrt{E\ (\rm GeV)} \oplus 50\ {\rm ps}$, respectively. The KLOE trigger [12] uses calorimeter and chamber information. For this analysis only the calorimeter signals are relevant. Two energy deposits with $E > 50$ MeV for the barrel and $E > 150$ MeV for the endcaps are required.

Prompt photons are identified as neutral particles with $\beta = 1$ originated at the interaction point requiring $|T - R/c| < \min(5\sigma_T, 2\ {\rm ns})$, where T is the photon flight time and R the path length; σ_T includes also the contribution of the bunch length jitter. The photon detection efficiency is $\sim 90\%$ for E_γ=20 MeV, and reaches 100% above 70 MeV. The sample selected by the timing requirement containes a $< 1.8\%$ contamination due to accidental clusters from machine background.

Table 1: Background channels for $\phi \to \pi^0\pi^0\gamma$.

Channel	S/B	Rejection Factor	Expected events
$\omega\pi$	0.80	8.7	339 ± 24
$\eta\pi\gamma$	3.52	4.0	166 ± 16
$\eta\gamma$	0.027	5.9×10^3	159 ± 12

1 Event selection

Two amplitudes contribute to $\phi \to \pi^0\pi^0\gamma$: $\phi \to S\gamma$, $S \to \pi^0\pi^0$ ($S\gamma$) and $\phi \to \rho^0\pi^0$, $\rho^0 \to \pi^0\gamma$ ($\rho\pi$) where S is a scalar meson.The event selection criteria of the $\phi \to \pi^0\pi^0\gamma$ decays ($\pi\pi\gamma$) have been designed to give similar efficiencies for both processes. The first step, requiring five prompt photons with $E_\gamma \geq$7 MeV and $\theta \geq \theta_{\min} = 23°$, reduces the sample to 124,575 events. The background due to $\phi \to K_S K_L$ is removed requiring that $E_{\rm tot} = \sum_5 E_{\gamma,i}$ and $\vec{p}_{\rm tot} = \sum_5 \vec{p}_{\gamma,i}$ satisfy $E_{\rm tot}$ >800 MeV and $|\vec{p}_{\rm tot}|$ <200 MeV/c. We are left with 15,825 events. Other reactions which give rise to background are: $e^+e^- \to \omega\pi^0 \to \pi^0\pi^0\gamma$ ($\omega\pi$), $\phi \to \eta\pi^0\gamma \to 5\gamma$ ($\eta\pi\gamma$) and $\phi \to \eta\gamma \to 3\pi^0\gamma$ ($\eta\gamma$) with 2 undetected photons. The ratio between signal and background rates is evaluated for these processes using the cross sections measured in the same data sample [13,14] and listed in Tab. 1.

A kinematic fit (Fit1) requiring overall energy and momentum conservation improves the energy resolution to 3%. Photons are assigned to π^0's by minimizing a test χ^2-function ($\chi^2_{\rm sel}$) for both the $\pi\pi\gamma$ and $\omega\pi$ cases. For the $\omega\pi$ case we also require $M_{\pi\gamma}$ to be consistent with M_ω. The correct combination is found by this procedure 89%, 96% of the time for the $\pi\pi\gamma$, $\omega\pi$ case respectively. Good agreement is found with the Monte Carlo simulation, MC, for the distributions of the χ^2 and of the invariant masses. A second fit (Fit2) requires the masses of $\gamma\gamma$ pairs to equal M_π. $\omega\pi$ is the largest background to $\pi\pi\gamma$ and the corresponding level of contamination must be determined. Similarly, $\pi\pi\gamma$ decay is the most relevant background to $\omega\pi$. The relative fraction of these decays are evaluated by an iterative procedure. The $\pi\pi\gamma$ simulation assumes only the $S\gamma$ process with a $\pi^0\pi^0$ mass (m) spectrum consistent with the data. In this paper we use the symbol $M_{\pi\pi}$ to denote the reconstructed value of m.

The search of $e^+e^- \to \omega\pi^0 \to \pi^0\pi^0\gamma$ retains events satisfying $\chi^2/{\rm ndf} \leq 3$ and $\Delta M_{\pi\gamma} = |M_{\pi\gamma} - M_\omega| \leq 3\,\sigma_\omega$ using Fit2 in the $\omega\pi$ hypothesis. Data and MC are in good agreement (Fig. 1.a-b). The $|\cos\psi|$ distribution, where ψ is the angle between γ and π^0 in the $\pi^0\pi^0$ frame, is shown in Fig. 1.c. Some disagreement is seen at large values of $|\cos\psi|$. Subtracting the MC background and integrating for $|\cos\psi|$ <0.8 we count

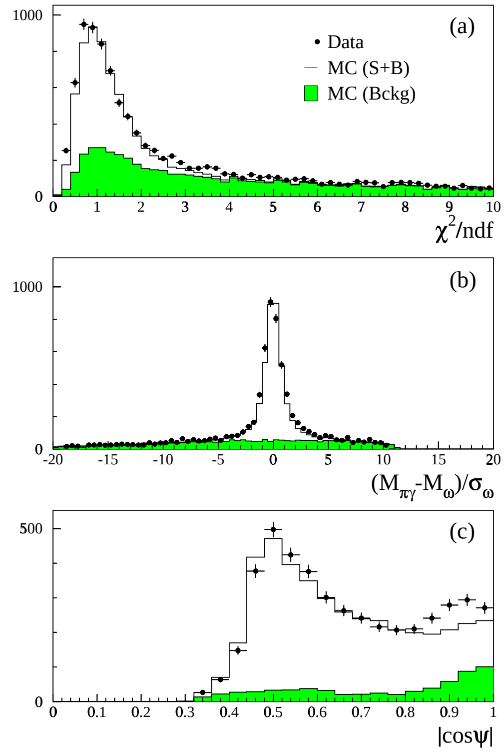

Figure 1: Data–MC comparison for $\omega\pi$ events: (a) χ^2/ndf; (b) $\Delta M_{\pi\gamma}/\sigma_\omega$ with $\chi^2/\mathrm{ndf} \leq 3$; (c) $|\cos\psi|$ distribution with $\chi^2/\mathrm{ndf} \leq 3$ and $|\Delta M_{\pi\gamma}|/\sigma_\omega \leq 5$.

2821±59 events. Accounting for efficiency ($\epsilon_{\omega\pi} = 38.2\%$) and normalizing to L_{int} we get $\sigma(\omega\pi) = (\,0.46 \pm 0.01_{\mathrm{stat}} \pm 0.03_{\mathrm{syst}}\,)\ \mathrm{nb}$. The systematic error accounts for the discrepancy with the MC for $|\cos\psi| > 0.8$ and for the error on the determination of L_{int} (2%).

After removing the $\omega\pi$ candidates, $\phi \to \pi^0\pi^0\gamma$ events must satisfy $\chi^2/\mathrm{ndf} \leq 3$ for Fit2 in the $\pi\pi\gamma$ hypothesis. We also require $\Delta M_{\gamma\gamma} = |M_{\gamma\gamma} - M_\pi| \leq 5\,\sigma_\pi$ using the photon momenta of Fit1. Background rejection factors are given in Tab. 1. The signal efficiency is $\epsilon_{\pi\pi\gamma} \sim 40\%$ and is shown in Fig. 2 as a function of $M_{\pi\pi}$. The $\rho\pi$ process shows similar behaviour. Fig. 3 shows various distributions for the 3102 events together with MC predictions. The angular distributions prove that $S\gamma$ is the dominant process. Subtracting the background of Tab. 1, 2438±61 $\phi \to \pi^0\pi^0\gamma$ events remain. Their $M_{\pi\pi}$ spectrum is shown in Fig. 4.

The systematic uncertainty on the number of $\pi\pi\gamma$ events originates from several effects, listed in the following. The error on the selection efficiency of five prompt photons

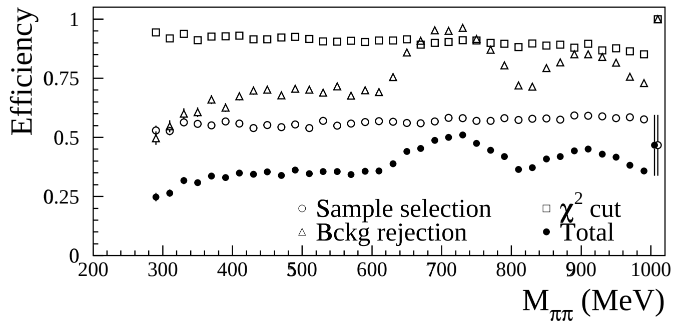

Figure 2: Efficiency vs $\pi^0\pi^0$ invariant mass for $\phi \to \pi^0\pi^0\gamma$ events. Individual contributions are also shown.

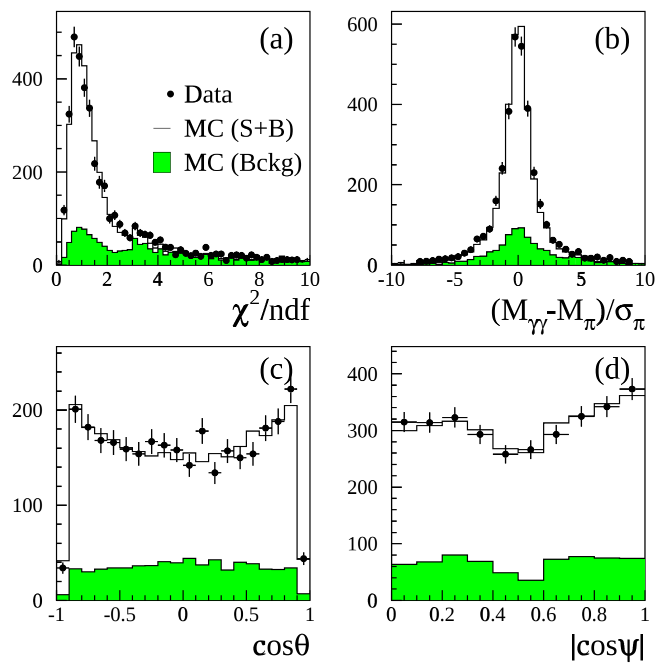

Figure 3: Data–MC comparison for $\phi \to \pi^0\pi^0\gamma$ events after $\omega\pi$ rejection: (a) χ^2/ndf; (b) $(M_{\gamma\gamma} - M_\pi)/\sigma_\pi$ with $\chi^2/\mathrm{ndf} \leq 3$; (c, d) angular distributions with all analysis cuts applied. θ is the polar angle of the radiative photon, ψ is the angle between the radiative photon and π^0 in the $\pi^0\pi^0$ rest frame.

is related to the simulation accuracy in describing the clustering. From a control sample of $\phi \to \eta\gamma \to \pi^0\pi^0\pi^0\gamma$ events, by comparing the cross section obtained using 7 or $6 + 7$ reconstructed clusters in the final state and extrapolating to five clusters, we obtain a relative systematic error of 1%. Residual effects due to analysis cuts were checked by varying the $\theta_{\rm min}$ and $\Delta M_{\gamma\gamma}$ cuts by $\pm 1^\circ$ and $\pm 1\sigma_\pi$ respectively; from the results we obtain a 2.0% systematic uncertainty.

2 A model for the spectrum of $M_{\pi\pi}$

In order to fit any model to the data, all effects distorting the observed mass spectrum $S_{\rm obs}(M_{\pi\pi})$ must be folded into the shape predicted by the model. In our case this involves the mass resolution and the effect of incorrect photon assignments. Our experimental response function is determined for a finite number of mass values.

The model spectrum $f(m)$ is taken as the sum of $S\gamma$, $\rho\pi$ and interference term, $f(m) = f_{S\gamma}(m) + f_{\rho\pi}(m) + f_{\rm int}(m)$. The scalar term is [4]:

$$f_{S\gamma}(m) = \frac{2\,m^2}{\pi}\,\frac{\Gamma_{\phi S\gamma}\Gamma_{S\pi^0\pi^0}}{|D_S|^2}\,\frac{1}{\Gamma_\phi}. \tag{1}$$

The $\phi \to S\gamma$ process is estimated by means of a K^+K^- loop for the f_0:

$$\Gamma_{\phi f_0\gamma}(m) = \frac{g^2_{f_0K^+K^-}\,g^2_{\phi K^+K^-}}{12\pi}\,\frac{|g(m)|^2}{M_\phi^2}\,\left(\frac{M_\phi^2 - m^2}{2M_\phi}\right), \tag{2}$$

where $g_{\phi K^+K^-}$ and $g_{f_0K^+K^-}$ are the couplings and $g(m)$ is the loop integral function.

A recent measurement [15] reports the existence of a scalar σ with $M_\sigma = (478^{+24}_{-23} \pm 17)$ MeV and $\Gamma_\sigma = (324^{+42}_{-40} \pm 21)$ MeV. If we include the contribution of this meson, with a $g_{\phi\sigma\gamma}$ coupling [16], we get:

$$\Gamma_{\phi\sigma\gamma}(m) = \frac{e^2\,g^2_{\phi\sigma\gamma}}{12\pi}\,\frac{1}{M_\phi^2}\,\left(\frac{M_\phi^2 - m^2}{2M_\phi}\right)^3. \tag{3}$$

$\Gamma_{S\pi^0\pi^0}$ is given by:

$$\Gamma_{S\pi^0\pi^0}(m) = \frac{1}{2}\,\Gamma_{S\pi^+\pi^-}(m) = \frac{g^2_{S\pi^+\pi^-}}{32\,\pi\,m}\,\sqrt{1 - \frac{4M_\pi^2}{m^2}}\,. \tag{4}$$

For the inverse propagator, D_S, we use the formula with finite width corrections [4] for the f_0 and a Breit Wigner for the σ. The parametrization of Ref. [17] has been used for the $\rho\pi$ and the interference term.

3 Results

Two different fits have been performed on $S_{\rm obs}(M_{\pi\pi})$ varying $f_{S\gamma}(m)$: in Fit (A) only the f_0 contribution is considered while in Fit (B) a mixing of f_0 and σ mesons is used.

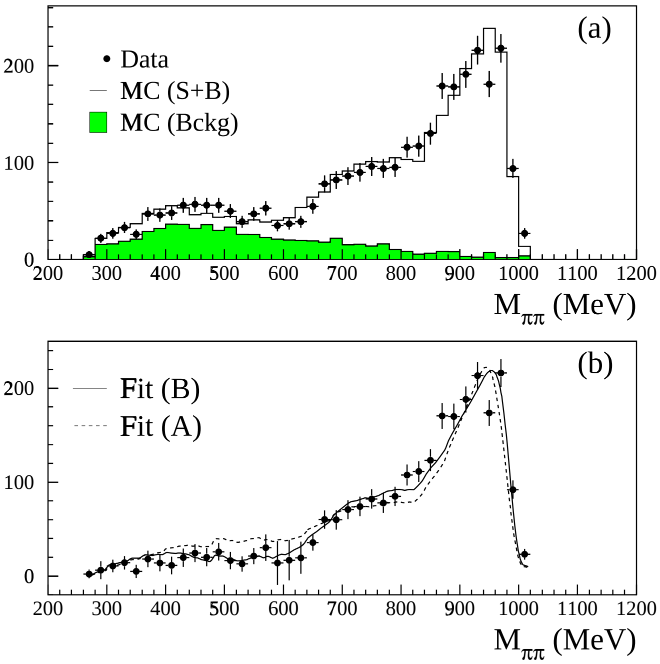

Figure 4: Observed spectrum of $\pi^0\pi^0$ invariant mass before (a) and after (b) background subtraction.

The mass and width of the σ were fixed to their central values. If the normalization of the $\rho\pi$ term is left free during fitting, its contribution and the related interference terms turn out to be negligibly small. When BR($\phi \to \rho^0\pi^0 \to \pi^0\pi^0\gamma$) is fixed at $1.8 \cdot 10^{-5}$ as in Ref. [17], the χ^2/ndf increases by more than a factor of 2. The fits without the $\rho\pi$ contribution are shown superimposed over the raw spectrum in Fig. 4.b.

Since Fit (B) agrees well with the data, it has been used to unfold $S_{\rm obs}(M_{\pi\pi})$. For each reconstructed mass bin, the ratio between the theoretical and the smeared function, $SF(M_{\pi\pi})$, is calculated. The normalized differential decay rate, $\mathrm{d}\text{BR}/\mathrm{d}m = (1/\Gamma)\mathrm{d}\Gamma/\mathrm{d}m$, is then given by:

$$\frac{\mathrm{d}\text{BR}}{\mathrm{d}m} = \frac{S_{\rm obs}(M_{\pi\pi})}{SF(M_{\pi\pi})}\,\frac{1}{L_{\rm int}\times\sigma(\phi)\times\Delta M_{\pi\pi}} \qquad (5)$$

For the normalization, the ϕ production cross section, $\sigma(\phi)$, was obtained from the $\phi \to \eta\gamma \to \gamma\gamma\gamma$ decay in the same sample [14]. The value of $\mathrm{d}\text{BR}/\mathrm{d}m$ as a function of m is given in Tab. 2 and shown in Fig. 5; the relative errors are given in Tab. 3.

Integrating over the whole mass range we obtain:

$$\text{BR}(\phi \to \pi^0\pi^0\gamma) = (1.09 \pm 0.03_{\rm stat} \pm 0.03_{\rm syst} \pm 0.04_{\rm norm}) \times 10^{-4}. \qquad (6)$$

Table 2: Differential BR for $\phi \to \pi^0\pi^0\gamma$. m is expressed in MeV while $\mathrm{dBR}/\mathrm{d}m$ is in units of $10^8\,\mathrm{MeV}^{-1}$. The errors listed are the total uncertainties.

m	$\frac{d\mathrm{BR}}{dm}$	m	$\frac{d\mathrm{BR}}{dm}$
290	2.0 ± 2.9	670	11.2 ± 1.9
310	2.2 ± 1.4	690	11.0 ± 1.9
330	3.0 ± 1.5	710	12.5 ± 1.9
350	0.9 ± 1.3	730	14.0 ± 2.0
370	2.9 ± 1.4	750	17.3 ± 2.3
390	2.2 ± 1.3	770	17.0 ± 2.4
410	1.4 ± 1.1	790	19.4 ± 2.5
430	1.8 ± 1.0	810	27.4 ± 3.1
450	1.9 ± 0.8	830	29.2 ± 3.2
470	1.1 ± 0.5	850	30.6 ± 3.2
490	0.5 ± 0.2	870	41.7 ± 3.8
510	0.2 ± 0.1	890	39.6 ± 3.6
530	0.3 ± 0.2	910	44.6 ± 3.8
550	1.3 ± 0.5	930	53.6 ± 4.4
570	3.3 ± 1.5	950	47.2 ± 4.3
590	2.1 ± 3.6	970	64.7 ± 5.3
610	3.7 ± 4.7	990	22.0 ± 2.5
630	4.2 ± 3.7	1010	0.2 ± 0.1
650	7.0 ± 1.7		

Table 3: Uncertainties on BR($\phi \to \pi^0\pi^0\gamma$).

Source	Relative error
Statistics	2.5%
Background	1.3%
Event counting	2.3%
Normalization	3.7%
Total	5.2%

Integrating in the f_0 dominated region, above 700 MeV:

$$\mathrm{BR}(\phi \to \pi^0\pi^0\gamma;\ m > 700\,\mathrm{MeV}) = (0.96 \pm 0.02_{\mathrm{stat}} \pm 0.02_{\mathrm{syst}} \pm 0.04_{\mathrm{norm}}) \times 10^{-4}.$$

The result of the fits are listed in Tab. 4. Fit (A) gives a larger χ^2 than Fit (B) and

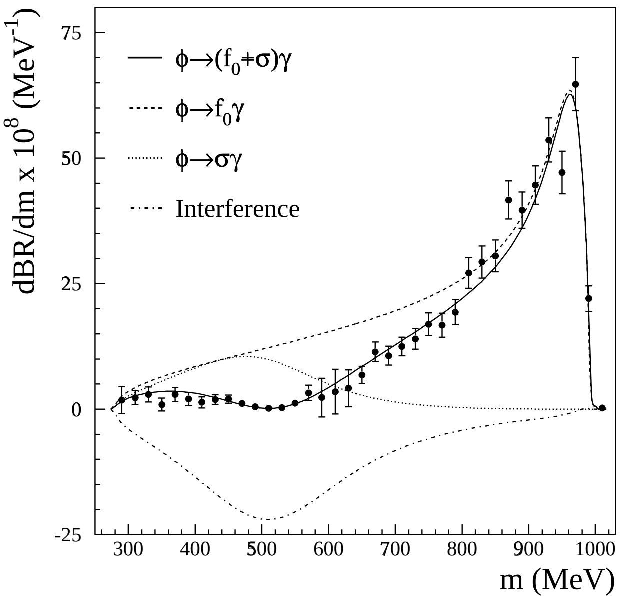

Figure 5: $\mathrm{dBR}/\mathrm{d}m$ as a function of m. Fit (B) is shown as a solid line; individual contributions are also shown.

yields lower values for the f_0 mass (M_{f_0}) and the coupling constants. In this case the BR($\phi \rightarrow f_0\gamma \rightarrow \pi^0\pi^0\gamma$) is $(1.11 \pm 0.06_{\mathrm{stat+syst}}) \times 10^{-4}$.

The best agreement with data is given by Fit (B), where the negative interference between the f_0 and σ amplitudes results in the observed decrease of the $\pi^0\pi^0\gamma$ yield below 700 MeV. In Fig. 5 the contributions from each individual term are also shown. Integrating over the f_0 and σ curves we obtain BR($\phi \rightarrow f_0\gamma \rightarrow \pi^0\pi^0\gamma$) $= (1.49 \pm 0.07_{\mathrm{stat+syst}}) \times 10^{-4}$ and BR($\phi \rightarrow \sigma\gamma \rightarrow \pi^0\pi^0\gamma$) $= (0.28 \pm 0.04_{\mathrm{stat+syst}}) \times 10^{-4}$.

The values of the coupling constants from Fit (B) are in agreement with those reported by the SND and CMD-2 experiments [2,3]. The coupling constants differ from the WA102 result on f_0 production in central pp collisions ($g^2_{f_0K^+K^-}/g^2_{f_0\pi^+\pi^-} = g_K/1.33\, g_\pi = 1.63 \pm 0.46$) [18] and from those obtained when the f_0 is produced in $D_s^+ \rightarrow \pi^+\pi^-\pi^+$ decays [19], where g_K is consistent with zero.

In a separate paper [13], we present a measurement of BR($\phi \rightarrow a_0\gamma$), together with a discussion of the implications of f_0 and a_0 results.

Table 4: Fit results using f_0 only (A) and f_0–σ mixing (B).

	Fit (A)	Fit (B)
χ^2/ndf	$109.53/34$	$43.15/33$
M_{f_0} (MeV)	962 ± 4	973 ± 1
$g^2_{f_0 K^+K^-}/(4\pi)$ (GeV^2)	1.29 ± 0.14	2.79 ± 0.12
$g^2_{f_0 K^+K^-}/g^2_{f_0\pi^+\pi^-}$	3.22 ± 0.29	4.00 ± 0.14
$g_{\phi\sigma\gamma}$	—	0.060 ± 0.008

Acknowledgements

We thank the DAΦNE team for their efforts in maintaining low background running conditions and their collaboration during all data-taking. We also thank F. Fortugno for his efforts in ensuring good operations of the KLOE computing facilities. We thank R. Escribano for discussing with us the existing theoretical framework. This work was supported in part by DOE grant DE-FG-02-97ER41027; by EURODAPHNE, contract FMRX-CT98-0169; by the German Federal Ministry of Education and Research (BMBF) contract 06-KA-957; by Graduiertenkolleg 'H.E. Phys.and Part. Astrophys.' of Deutsche Forschungsgemeinschaft, Contract No. GK 742; by INTAS, contracts 96-624, 99-37; and by TARI, contract HPRI-CT-1999-00088.

References

[1] M.N. Achasov *et al.*, Phys. Lett. B 440 (1998) 442.

[2] M.N. Achasov *et al.*, Phys. Lett. B 485 (2000) 349.

[3] R.R. Akhmetshin *et al.*, Phys. Lett. B 462 (1999) 380.

[4] N.N. Achasov and V.N. Ivanchenko, Nucl. Phys. B 315 (1989) 465.

[5] N.A. Törnqvist, Phys. Rev. Lett. 49 (1982) 624.

[6] R.L. Jaffe, Phys. Rev. D 15 (1997) 267.

[7] J. Weinstein and N. Isgur, Phys. Rev. Lett. 48 (1982) 659.

[8] KLOE Collaboration, LNF-92/019 (IR) (1992) and LNF-93/002 (IR) (1993).

[9] S. Guiducci *et al.*, Proc. of the 2001 Particle Accelerator Conference (Chicago, Illinois, USA), P. Lucas S. Webber Eds., 2001, 353.

[10] KLOE Collaboration, M. Adinolfi *et al.*, LNF Preprint LNF-01/016 (IR) (2001), accepted by Nucl. Inst. and Meth.

[11] KLOE Collaboration, M. Adinolfi *et al.*, Nucl. Inst. and Meth. A 482 (2002) 363.

[12] KLOE Collaboration, M. Adinolfi *et al.*, LNF Preprint LNF-02/002 (P) (2002), submitted to Nucl. Inst. and Meth.

[13] KLOE Collaboration, A. Aloisio *et al.*, submitted to Phys. Lett. B.

[14] S. Giovannella and S. Miscetti, KLOE Note 177, April 2002.

[15] E.M. Aitala *et al.*, Phys. Rev. Lett. 86 (2001) 770.

[16] A. Gokalp and O. Yilmaz, Phys. Rev. D 64 (2001) 053017 and private communication.

[17] N.N. Achasov and V.V. Gubin, Phys. Rev. D 63 (2001) 094007.

[18] D. Barberis *et al.*, Phys. Lett. B 462 (1999) 462; F.E. Close A. Kirk, Phys. Lett. B 515 (2001) 13.

[19] E.M. Aitala *et al.*, Phys. Rev. Lett. 86 (2001) 765.